applied sciences

MDPI

Article

Toward Gas-Phase Thermometry Using Pure-Rotational Impulsive Stimulated Raman Scattering Spectroscopy with a Low-Energy Femtosecond Oscillator

Mauro Falconieri [1,*], Davide Tedeschi [1], Serena Gagliardi [1], Flaminia Rondino [1], Michele Marrocco [1] and Waruna D. Kulatilaka [2]

[1] ENEA, C.R. Casaccia, Via Anguillarese 301, 00123 Roma, Italy
[2] J. Mike Walker'66 Department of Mechanical Engineering, Texas A&M University, College Station, TX 77843, USA
* Correspondence: mauro.falconieri@enea.it

Abstract: Femtosecond coherent Raman techniques have significant diagnostic value for the sensitive and non-intrusive measurement of temperature, pressure, and composition of gas mixtures. Due to the low density of samples, however, such measurements make use of high-energy amplified laser sources, with unwieldy and costly experimental setups. In this paper, we demonstrate an experimental setup equipped with a low-energy and low-average-power femtosecond oscillator allowing measurement of the pure-rotational spectrum of nitrogen down to atmospheric pressure using impulsive stimulated Raman scattering. Using a simplified model to analyze the experimental data we were able to derive the gas temperature with reasonable accuracy.

Keywords: impulsive stimulated Raman scattering (ISRS); rotational spectroscopy; gas-phase diagnostics

Citation: Falconieri, M.; Tedeschi, D.; Gagliardi, S.; Rondino, F.; Marrocco, M.; Kulatilaka, W.D. Toward Gas-Phase Thermometry Using Pure-Rotational Impulsive Stimulated Raman Scattering Spectroscopy with a Low-Energy Femtosecond Oscillator. *Appl. Sci.* **2022**, *12*, 12710. https://doi.org/10.3390/app122412710

Academic Editor: Bernhard Wilhelm Roth

Received: 10 November 2022
Accepted: 9 December 2022
Published: 11 December 2022

1. Introduction

Coherent Raman spectroscopy of gas-phase rotational wave packets was demonstrated to be a valuable tool for the characterization of temperature, pressure, and composition of gas mixtures. Since molecular rotational spectra are extremely sensitive to the environment, the associated Raman coherence generated with ultrashort laser pulses is commonly used in coherent anti-Stokes Raman scattering (CARS) experiments applied to reacting gases to determine the physical and chemical conditions [1–6].

Coherent rotational wave packets can also be studied using the alternative technique of stimulated Raman scattering (SRS), and particularly using the impulsive excitation scheme (ISRS), in which excitation of the rotational Raman modes is attained by an ultrafast pump pulse with a duration much shorter than the smaller relevant Raman period [7,8]. This condition translates into easy access to the low-frequency Raman region (<500 cm^{-1}), with commercially available ultrafast sources [9], and for this reason, it is captivating to answer the question of whether the diagnostic capability of CARS can be extended to impulsive SRS. In general, SRS has several advantages over CARS. Among them, the most important difference is in the dependence on dielectric susceptibility ($|\chi|^2$ for CARS, whereas Im(χ) for SRS), which results in simpler SRS spectra reproducing those obtained via spontaneous (i.e., linear) Raman. In addition, phase matching is inessential in SRS whereas it troubles CARS arrangements [10]. Moreover, ISRS is realized with a single ultrafast laser beam and a relatively simple setup [11,12], while single-beam configurations available for CARS [13,14] need sophisticated sectioning of the spectral content of the laser. As a matter of fact, ISRS was demonstrated in low-frequency Raman characterization of condensed-phase samples in setups equipped with a single low-energy femtosecond source with improved data acquisition rate [15,16] and signal-to-noise ratio (SNR) [12,15–18], allowing the realization

of video-rate low-frequency Raman microscopes [18]. On the other hand, low-excitation energy ISRS has never been demonstrated in the gas phase to the best of our knowledge. Low-energy fs pulses in the range of 80 MHz can be easily obtained using a compact commercial fs oscillator as opposed to more complex kHz-rate amplified fs lasers used in gas-phase CARS thermometry.

The commonly adopted ISRS setup is based on a Fourier-transform (FT) spectrometer [9,12,19], where the sample polarization associated with the vibrational coherent state established by an ultrashort pump pulse interferes with a second, delayed ultrashort (probe) pulse, producing modifications which are detected as a signal. The signal is recorded as a function of the pump–probe delay and is therefore modulated with the same period of the vibrational coherent polarization. An FT of the delay-dependent signal finally gives the frequency spectrum of the vibrational modes. As far as the nature of the signal is concerned, the interference of the probe beam with the sample Raman polarization results in both spectral and refractive effects caused by the occurrence of stimulated Raman gain/loss phenomena and of the Raman-induced Kerr effect [11,19]. The characteristics and the relative magnitude of these two types of signals were discussed in [17,19] and more recently reviewed in [9].

In the gas phase, the coherent excitation of nearly equally spaced rotational levels of the sample produces periodic, isolated transients (rotational revivals) at fractional multiples of the fundamental rotational period, due to the recurrent realignment of the molecules. The resulting birefringence was exploited in the so-called Raman-induced polarization spectroscopy (RIPS) technique [20–23] to study the rotational dynamics and to measure the concentration of gases in mixtures, in layouts equipped with high-energy amplified ultrashort laser sources. RIPS was also used to measure the temperature of mixtures of gases by comparing the time-domain signal shape with the predictions of available collisional models [24]. Rotational wave packets were also measured by detection of the probe beam deflection [25] using high-energy excitation, with amplified sources delivering from several hundred microjoules to several millijoules. All the above-cited works detect the refractive effect of the rotational coherence, even though spectral effects were also measured and modeled by measuring the probe spectrum at selected pump–probe delay times [8,26,27]. However, to the best of our knowledge, the time-dependent spectral ISRS signal showing the rotational revivals structure has never been reported before.

In this paper, we show that a suitably arranged ISRS setup with spectral detection, equipped with a single-oscillator ultrashort source delivering few nanojoule energy and less than a milliwatt average power, can be used to measure the rotational wave packet revivals in N_2 at different pressures, with a measurement time down to 100 s. From these measurements, we obtain a low-resolution rotational spectrum of the sample, which we use to derive the temperature with a certain accuracy without the need for collisional linewidth models. While these values might still not be suitable for practical use of the technique, they are not limited by intrinsic or fundamental issues, and therefore can be substantially improved by the further tuning of the components of the experimental setup. We believe these findings pave the way for low-cost exploitation of coherent pure-rotational spectroscopy of gases, with important applications ranging from fundamental molecular physics studies to remote, non-intrusive, temperature measurements.

2. Materials and Methods

The experimental apparatus is an FT ISRS spectrometer based on a Michelson interferometer with orthogonally polarized beams in the two arms acting as pump and probe, see Figure 1.

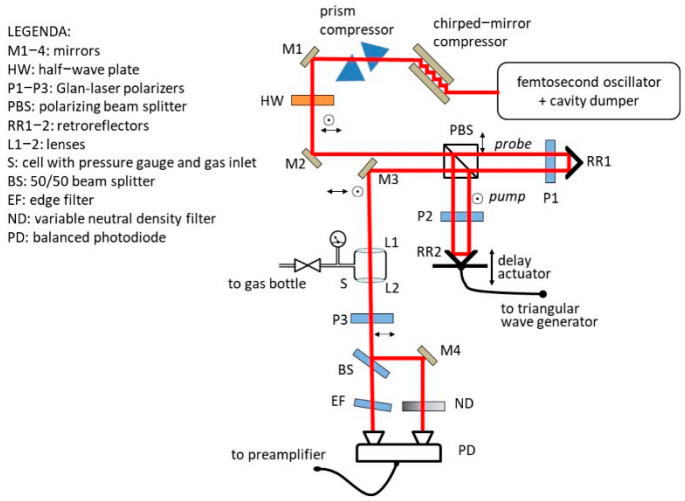

Figure 1. Experimental layout.

The two beams are produced from a single polarized laser source by means of a half-wave plate and a polarizing beam splitter; the half-wave plate is also used to control the pump/probe energy ratio, which is set to 10:3 in the present experiments. The laser beam is provided by a cavity-dumped femtosecond oscillator (Coherent MIRA 900F, Santa Clara, CA, USA; plus PulseSwitch, APE GmbH, Berlin, Germany) operating at 780 nm with typical pulse energy equal to about 18 nJ, 40 kHz repetition rate and 12 nm bandwidth. The 12 nm bandwidth allows for impulsive excitation of Raman modes below approximately 200 cm^{-1}. Before the interferometer, the beam is pre-treated by two compressors, a chirped-mirrors one (DCMP 175, Thorlabs GmbH Bergkirchen, Germany) and a double-pass prism one, to compensate for the laser chirp and for the layout optics dispersion, allowing to obtain a minimum autocorrelator pulse width at the sample position equal to 106 fs, corresponding to a Gaussian 1/e pulse width $\tau_G \cong 44$ fs. One of the interferometer arms (the pump beam one) is equipped with a retroreflector mounted on a rapid scanning actuator (a loudspeaker) capable of producing a periodically modulated delay of more than 12 ps with a frequency of few tens of Hertz. In the experiments, the delay is modulated by a triangular waveform whose amplitude and frequency were experimentally optimized for extended delay range and linear loudspeaker excursion; moreover, the loudspeaker rest position is adjusted so that the modulation causes the pump pulses to arrive from slight delay to substantial advance with respect to the probe pulse. The fast periodic delay modulation is necessary to implement the signal averaging by delay-scan [18,28], a noise reduction technique that was demonstrated to be advantageous over fixed-point averaging. The pump and probe beams recombine at the beam splitter and are sent to the sample by a 2.5 cm focal length lens; then, beams are recollimated by a second lens with the same focal length after the sample. The two lenses are mounted as windows of a homemade stainless-steel cell with a removable cap allowing access to the main lens focus position. For calibration purposes, a 0.1 cm quartz cuvette containing a liquid reference sample can be inserted in the cell in the focal position of the lenses, while for gas-phase measurements, the cell is evacuated and filled with pure N_2 at a controlled pressure. After the sample, the probe beam is singled out by a Glan-laser polarizer (P3) and is sent to the detection assembly. Note that to minimize the pump leakage on the probe beam, the polarization purity of the two beams in the interferometer is enforced by using a Glan laser polarizer in each arm (P1–P2).

As widely discussed in the literature [12,17,19], the probe beam is subjected to refractive and spectral effects due to the Raman coherent oscillations in the sample; in this experiment, we detect the ISRS-induced spectral shifts using the standard arrangement [11,19] consisting of an edge filter (LP02-780RU-25 Semrock, IDEX Health & Science, LLC, Rochester, NY, USA), tuned at the center wavelength of the probe, placed in front of one of the channels of a balanced photodiode detector (Thorlabs PBD210/A). To ensure

tuning at the actual center of the probe spectrum and thus maximize the spectral detection sensitivity [19], the edge filter is tilted in order to transmit approximately 50% of the probe beam intensity. A fraction of the probe beam (not spectrally filtered) is sent to the other channel of the balanced detector; this arrangement allows the reduction of the signal noise due to pulse-to-pulse and beam pointing fluctuations, and, by careful adjustment of the beam intensities using neutral density filters, to have a null DC baseline output in the absence of spectral shifts. The signal from the balanced detector is amplified (Femto DLPVA-100-B-S) and then digitalized by a low-cost USB ADC (USB1608 GX, Measurement Computing Corp., Norton, MA, USA) triggered by the laser cavity dumper electronics so that the signal is measured for each laser pulse. The ADC is controlled by a LabView program which measures and averages the signal as a function of time for a pre-set number of the scanning delay cycles in phase with the delay modulation so that for each cycle, two sets of delay-dependent signal points are measured, corresponding to the back-and-forth movement of the actuator.

Raw data were processed by averaging the two measurements and calibrating the time to obtain the true delay time. Since in this setup we do not employ a system for online real-time measurement of the pump–probe delay, in order to transform the signal measurement time into a calibrated delay scale, we used the signal of a standard CH_2Br_2 sample which shows weakly damped, equally spaced oscillations with a period of 193 fs corresponding to the known Raman resonance at 173 cm^{-1} due to the Br-C-Br bending mode [29]. In this way, we were able to calibrate the pump–probe delay up to more than 12 ps, accounting also for small nonlinearities of the delay actuator movement.

3. Results

Measurements were performed as a function of the N_2 pressure in the cell in the range of 1–10 atm. The time-dependent spectral ISRS signals measured at different N_2 pressures using an integration time equal to 100 s, corresponding to 2000 signal averages, are shown in Figure 2a.

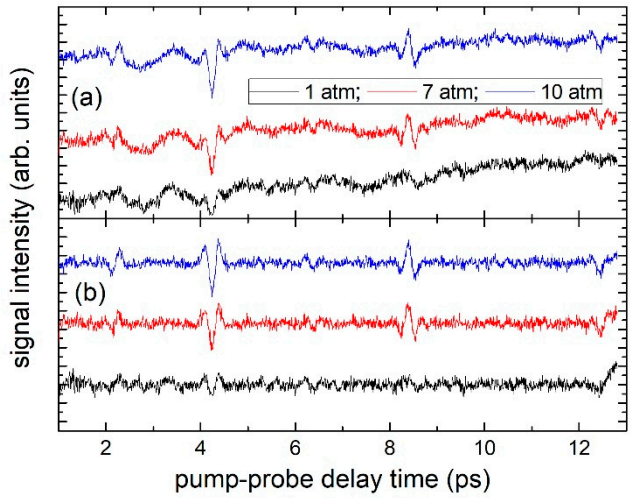

Figure 2. (**a**) Time-dependent ISRS signals measured in N_2 at different pressures. (**b**) Same as (**a**) after FT filtering (see text).

Clear rotational wave packet interference revivals can be seen at around 2, 4, 8, and 12 ps, especially for the measurements at the highest pressure; however, the signal is detectable down to atmospheric pressure. The positions of the observed revivals are in agreement with published data measured using amplified femtosecond sources [25,30]. However, the shape of the revivals is different from that reported in previous studies since here we are detecting the spectral ISRS signal. In particular, we can observe that each signal can be described as an alternate of revivals, which can be labeled according to their shape

as "dispersion"- or "peak"-like, the two shapes being connected by a derivative. Therefore, since the spectral ISRS signal is proportional to the derivative of its refractive counterpart, our data show a revival pattern that is complementary to those reported before.

From Figure 2a it can be seen that the revival signals sit on a slowly variable background which does not scale with the sample pressure and is due to a systematic experimental artifact produced by the delay scan mechanism, as verified on a CH_2Br_2 reference sample. This background can be removed by post-acquisition data processing, e.g., by a 1 THz high-pass FT filter, obtaining much clearer signals as shown in Figure 2b. It is interesting to observe that the dependence of the signal intensity on the sample pressure is not trivial. Notwithstanding the well-known linearity of the SRS signal on sample concentration in condensed matter samples, in the gas phase, many phenomena concur to alter this situation. For example, in femtosecond CARS measurements, the signal dependence on sample concentration is almost linear [14] in the gas phase, differently from the usual quadratic behavior in condensed matter. Accordingly, we expect a sublinear, almost square-root, dependence of the signal intensity on the gas pressure. It is worth observing that improvement of the SNR can be achieved by increasing the laser repetition rate, which improves the statistics of the measurements. In the present experiment, the laser repetition rate is limited to 40 kHz in order to demonstrate a low-average power (<1 mW) operation, but, for example, using a 1 MHz repetition rate (which is a typical maximum figure for a cavity dumper) an SNR improvement of factor five ($\sqrt{10^6/4{\cdot}10^3}$) can be foreseen, with a limited average power of only 18 mW, well below the levels commonly used in spontaneous Raman measurements (several hundreds of mW). The use of a higher repetition rate, providing a higher number of pulses during the scan, enables the use of faster delay scan mechanisms [31], thus allowing a shorter measurement time at a fixed number of averages. An experimental implementation of these features will be the subject of future work.

As known, the Raman spectrum of the sample can be obtained by a fast Fourier transform (FFT) of the time-dependent ISRS signal; the results of this operation on the data shown in Figure 2b are reported in Figure 3a.

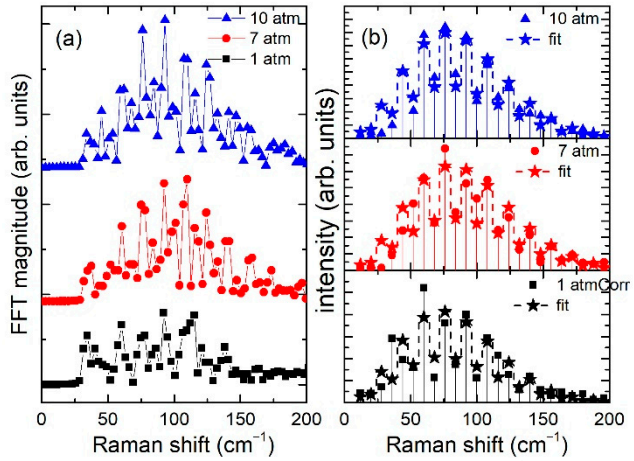

Figure 3. (**a**) Magnitude of the FFT of the ISRS data shown in Figure 2b. (**b**) Raman spectra of N_2 samples at different pressures obtained by division of the FFT data shown in (**a**) by the Raman shift and interpolation on the N_2 rotational lines, together with fits of the line intensities calculated as described in the text.

The rotational levels of N_2 are visible in the region 50–150 cm^{-1} even in the sample at atmospheric pressure and are quite evident in measurements at 7 and 10 atm. The resolution of the data shown in Figure 3a is slightly worse than 2.5 cm^{-1} and is due to the available maximum delay. Considering that the rotational line spacing of N_2 ($\Delta\omega = 4B \cong 8$ cm^{-1}, with the rotational constant $B \cong 1.99$ cm^{-1} [32]) is larger than the resolution and that the linewidth is almost constant and much smaller (order of tenths of cm^{-1}), this lack

of resolution is an instrumental effect which does not alter the relative intensities of the rotational lines. On the other hand, the resolution could be improved by using different delay scan layouts; improvement of the delay scan mechanism is also likely to increase the SNR, eliminating background signal fluctuations. However, given the N_2 linewidth, the measurement of a full-resolution spectrum would be feasible only by realizing very long delays with a motorized delay stage, impairing the use of delay-average noise-reduction techniques. Moreover, the long-time rotational revivals were shown to be affected by pressure-dependent energy transfer effects that alter the initial rotational coherence [33,34] and consequently the derived rotational spectral intensities. In this case, the use of experimental data to obtain information on the sample pressure or temperature requires apposite models whose development and suitability are still under debate [33,35]. Therefore, measurements at short delay times have significance since they represent an instantaneous picture of the rotational coherence created by the pump pulse.

4. Discussion

To clarify the above point in a simple way, we observe that the slow (Raman) nonlinearity created by an ultrafast pulse can be written as [8,36,37]:

$$\delta n_R(t) = \int_0^\infty R(\vartheta) I(t-\vartheta) d\vartheta \tag{1}$$

where $R(\vartheta)$ is the Raman response function of the sample and $I(t)$ is the pump pulse intensity. $R(\vartheta)$ was repeatedly modeled in the literature [8,9,37] as a sum of contributions of molecular rotational transitions:

$$R(\vartheta) \propto \sum_J F_J \sin\left(2\pi c \omega_J \vartheta\right) \tag{2}$$

where c is the speed of light; J is the rotational quantum number; $\omega_J = 2B(2J+3)$ are the rotational wavenumbers of a rigid rotator with B the rotational constant of the molecule; and F_J are the line intensities, given by:

$$F_J = \left(\rho_{J+2} - \rho_J\right) Z_J (J+2)(J+1)/(2J+3) \tag{3}$$

in which:

$$\rho_J = \frac{\exp[-chBJ(J+1)/kT]}{\sum_J Z_J (2J+1)\exp[-chBJ(J+1)/kT]}, \tag{4}$$

h is the Planck constant; k is the Boltzmann constant; T is the temperature; and Z_J is a degeneracy factor due to nuclear spin. Evaluation of (3) for N_2 at room temperature shows that above J = 23 ($\omega_J \cong 187$ cm^{-1}), the relative population of rotational modes is less than 0.05. The corresponding rotational period ($T_{JMAX} \cong 170$ fs) is longer than the laser pulse width ($\tau_G \cong 44$ fs) in our experiment, allowing us to conclude that, as a first approximation, the pump pulse can be considered instantaneous with respect to molecular rotations, and thus its temporal distribution can be approximated as a delta function in the convolution (1), giving $\delta n_R(t) \approx R(t)$. The same approximation applies to the probe pulse, which substantially senses the instantaneous Raman response of the sample.

Since the rotational intensities (3) depend on the temperature, the above equations can be used to analyze the experimental data reported in Figure 3a to derive the sample temperature. For a meaningful comparison, however, the data must be interpolated on the rotational frequencies ω_J and corrected for the proportional dependence of the ISRS spectral signal on the wavenumber [11,19]. The resultant Raman spectra are shown in Figure 3b, together with the fits obtained using the model expression (3) for F_J with the temperature and an overall normalization constant as fitting parameters. The best-fitting temperatures are 238 ± 20, 289 ± 19, and 265 ± 13 K for 1, 7, and 10 atm N_2 pressure, respectively, which are to be compared with the room temperature T = 295 K. The larger deviation of the fitted temperature at 1 atm from the actual value is clearly produced by

the poor SNR, a figure that can be improved as discussed above. Noticeably, the fitting temperatures tend to be systematically lower than the actual value, an effect which can be due to the reduced excitation of the higher-energy rotational levels resulting from a non-sufficiently short pump pulse. This effect could be accounted for by relaxing the approximation of purely impulsive excitation, e.g., calculating the integral (1) using a functional form for the laser pulse intensity different from the delta function. On the other hand, a simplified approach to compensate for this effect is to correct the experimental data by dividing by an excitation efficiency factor $\exp\left(-\omega^2\tau_G^2/4\right)$ [11]. Applying this correction, the new fitting temperatures are 264 ± 23, 321 ± 20, and 291 ± 14 K, for 1, 7, and 10 atm N_2 pressure, respectively, in satisfactory agreement with the actual value notwithstanding the simplifications and approximations involved in the data analysis.

It is worth observing that the assumption of purely impulsive excitation depends on the ratio of the laser pulse width τ_G to the rotation period of the highest populated rotational level T_{JMAX}. Since this occupation depends on the temperature, an increasingly shorter pulse width is necessary when increasing sample temperatures for the approximation to hold. In our experiment, the ratio $\frac{\tau_G}{T_{JMAX}}$ is equal to 0.26, and, keeping this figure as a minimum requirement, using the model above we can calculate that at T = 2000 K, the necessary pulse width is about 18 fs, which is attainable with modern commercial femtosecond oscillators. Therefore, the experimental setup demonstrated in this paper holds the promise of applicability to high-temperature and combustion diagnostics.

5. Conclusions

The data reported in this manuscript demonstrate the measurements of pure-rotational Raman spectra in N_2 using the spectral effects of impulsive stimulated Raman scattering, with an experimental setup equipped with a single cavity-dumped femtosecond oscillator. The laser pulse energy is a few nanojoules at a 40 kHz repetition rate, corresponding to an average power of a fraction of mW. The spectral resolution and the SNR of the data are sufficient to estimate the sample temperature using a simplified model for data analysis. Up to now, similar measurements were performed using several tens of thousand times higher energy (order of millijoules) for coherent techniques, and several thousand times higher average power (several hundred milliwatts) for the spontaneous Raman counterparts. Considering that the signal quality can be improved using a number of straightforward ways already outlined above, our findings could be useful for easy access to time-resolved rotational spectroscopy, as well as for other applications such as thermometry in remote or hazardous areas.

Author Contributions: Conceptualization, M.F.; methodology, M.F.; software, M.F.; validation, M.F., S.G. and M.M.; formal analysis, M.F.; investigation, D.T., M.F., S.G., F.R. and M.M.; resources, M.F., S.G. and F.R.; data curation, D.T., M.F. and W.D.K.; writing—original draft preparation, M.F.; writing—review and editing, D.T., S.G., F.R., M.M. and W.D.K.; visualization, D.T., S.G., F.R., M.M. and W.D.K.; supervision, M.F.; project administration, M.F.; funding acquisition, M.F. All authors have read and agreed to the published version of the manuscript.

Funding: This research was co-funded by the Italian Ministry of Foreign Affairs and International Cooperation (MAECI), under the Italy–USA Great Relevance Project "Spettrometro Raman coerente al femtosecondo a bassi numeri d'onda".

Institutional Review Board Statement: Not applicable.

Informed Consent Statement: Not applicable.

Data Availability Statement: Data are available from the corresponding author upon reasonable request.

Acknowledgments: The authors gratefully acknowledge the help of Giuliano Guidarelli in realizing the gas cell.

Conflicts of Interest: The authors declare no conflict of interest. The funders had no role in the design of the study; in the collection, analyses or interpretation of data; in the writing of the manuscript; or in the decision to publish the results.

References

1. Roy, S.; Gord, J.R.; Patnaik, A.K. Recent advances in coherent anti-Stokes Raman scattering spectroscopy: Fundamental developments and applications in reacting flows. *Prog. Energy Combust. Sci.* **2010**, *36*, 280–306. [CrossRef]
2. Miller, J.D.; Roy, S.; Slipchenko, M.N.; Gord, J.R.; Meyer, T.R. Single-shot gas-phase thermometry using pure-rotational hybrid femtosecond/picosecond coherent anti-Stokes Raman scattering. *Opt. Express* **2011**, *19*, 15627–15640. [CrossRef] [PubMed]
3. Stauffer, H.U.; Miller, J.D.; Slipchenko, M.N.; Meyer, T.R.; Prince, B.D.; Roy, S.; Gord, J.R. Time- and frequency-dependent model of time-resolved coherent anti-Stokes Raman scattering (CARS) with a picosecond-duration probe pulse. *J. Chem. Phys.* **2014**, *140*, 024316. [CrossRef] [PubMed]
4. Kearney, S.P. Hybrid fs/ps rotational CARS temperature and oxygen measurements in the product gases of canonical flat flames. *Combust. Flame* **2015**, *162*, 1748–1758. [CrossRef]
5. Kearney, S.P.; Danehy, P.M. Pressure measurements using hybrid femtosecond/picosecond rotational coherent anti-Stokes Raman scattering. *Opt. Lett.* **2015**, *40*, 4082–4085. [CrossRef]
6. Richardson, D.R.; Stauffer, H.U.; Roy, S.; Gord, J.R. Comparison of chirped-probe-pulse and hybrid femtosecond/picosecond coherent anti-Stokes Raman scattering for combustion thermometry. *Appl. Opt.* **2017**, *56*, E37–E49. [CrossRef]
7. Nibbering, E.; Grillon, G.; Franco, M.A.; Prade, B.S.; Mysyrowicz, A. Determination of the inertial contribution to the nonlinear refractive index of air, N_2, and O_2 by use of unfocused high-intensity femtosecond laser pulses. *J. Opt. Soc. Am. B* **1997**, *14*, 650–660. [CrossRef]
8. Ripoche, J.F.; Grillon, G.; Prade, B.; Franco, M.; Nibbering, E.; Lange, R.; Mysyrowicz, A. Determination of the time dependence of n2 in air. *Opt. Commun.* **1997**, *135*, 310–314. [CrossRef]
9. Bartels, R.A.; Oron, D.; Rigneault, H. Low frequency coherent Raman spectroscopy. *J. Phys. Photonics* **2021**, *3*, 042004. [CrossRef]
10. Rigneault, H.; Berto, P. Coherent Raman light matter interaction processes. *APL Photonics* **2018**, *3*, 091101. [CrossRef]
11. Yan, Y.-X.; Gamble, E.B.; Nelson, K.A. Impulsive stimulated scattering: General importance in femtosecond laser pulse interactions with matter, and spectroscopic applications. *J. Chem. Phys.* **1985**, *83*, 5391–5399. [CrossRef]
12. Raanan, D.; Ren, L.; Oron, D.; Silberberg, Y. Impulsive Raman spectroscopy via precision measurement of frequency shift with low energy excitation. *Opt. Lett.* **2018**, *43*, 470–473. [CrossRef] [PubMed]
13. Roy, S.; Wrzesinski, P.; Pestov, D.; Gunaratne, T.; Dantus, M.; Gord, J.R. Single-beam coherent anti-Stokes Raman scattering spectroscopy of using a shaped 7 fs laser pulse. *Appl. Phys. Lett.* **2009**, *95*, 074102. [CrossRef]
14. Roy, S.; Wrzesinski, P.J.; Pestov, D.; Dantus, M.; Gord, J.R. Single-beam coherent anti-Stokes Raman scattering (CARS) spectroscopy of gas-phase CO_2 via phase and polarization shaping of a broadband continuum. *J. Raman Spectrosc.* **2010**, *41*, 1194–1199. [CrossRef]
15. Peterson, W.; Hiramatsu, K.; Goda, K. Sagnac-enhanced impulsive stimulated Raman scattering for highly sensitive low-frequency Raman spectroscopy. *Opt. Lett.* **2019**, *44*, 5282–5285. [CrossRef]
16. Peterson, W.; Gala de Pablo, J.; Lindley, M.; Hiramatsu, K.; Goda, K. Ultrafast impulsive Raman spectroscopy across the terahertz–fingerprint region. *Adv. Photon.* **2022**, *4*, 016003. [CrossRef]
17. Falconieri, M.; Gagliardi, S.; Rondino, F.; Marrocco, M.; Kulatilaka, W.D. High-sensitivity impulsive stimulated Raman spectrometer with fast data acquisition. *J. Raman Spectrosc.* **2021**, *52*, 664–669. [CrossRef]
18. Raanan, D.; Audier, X.; Shivkumar, S.; Asher, M.; Menahem, M.; Yaffe, O.; Forget, N.; Rigneault, H.; Oron, D. Sub-second hyper-spectral low-frequency vibrational imaging via impulsive Raman excitation. *Opt. Lett.* **2019**, *44*, 5153–5156. [CrossRef]
19. Wahlstrand, J.K.; Merlin, R.; Li, X.; Cundiff, S.T.; Martinez, O.E. Impulsive stimulated Raman scattering: Comparison between phase-sensitive and spectrally filtered techniques. *Opt. Lett.* **2005**, *30*, 926–928. [CrossRef]
20. Lin, C.H.; Heritage, J.P.; Gustafson, T.K.; Chiao, R.Y.; McTague, J.P. Birefringence arising from the reorientation of the polarizability anisotropy of molecules in collisionless gases. *Phys. Rev. A* **1976**, *13*, 813–829. [CrossRef]
21. Morgen, M.; Price, W.; Hunziker, L.; Ludowise, P.; Blackwell, M.; Chen, Y. Femtosecond Raman-induced polarization spectroscopy studies of rotational coherence in O_2, N_2 and CO_2. *Chem. Phys. Lett.* **1993**, *209*, 1–9. [CrossRef]
22. Sarkisov, O.M.; Tovbin, D.G.; Lozovoy, V.V.; Gostev, F.E.; Titov, A.A.; Antipin, S.A.; Umanskiy, S.Y. Femtosecond Raman-induced polarisation spectroscopy of coherent rotational wave packets: D_2, N_2 and NO_2. *Chem. Phys. Lett.* **1999**, *303*, 458–466. [CrossRef]
23. Hertz, E.; Lavorel, B.; Faucher, O.; Chaux, R. Femtosecond polarization spectroscopy in molecular gas mixtures: Macroscopic interference and concentration measurements. *J. Chem. Phys.* **2000**, *113*, 6629–6633. [CrossRef]
24. Tran, H.; Lavorel, B.; Faucher, O.; Saint-Loup, R.; Joubert, P. Temperature measurement in gas mixtures by femtosecond Raman-induced polarization spectroscopy. *J. Raman Spectrosc.* **2003**, *34*, 994–998. [CrossRef]
25. Reichert, M.; Zhao, P.; Reed, J.M.; Ensley, T.R.; Hagan, D.J.; Van Stryland, E.W. Beam deflection measurement of bound electronic and rotational nonlinear refraction in molecular gases. *Opt. Express* **2015**, *23*, 22224–22237. [CrossRef]
26. Cai, H.; Wu, J.; Couairon, A.; Zeng, H. Spectral modulation of femtosecond laser pulse induced by molecular alignment revivals. *Opt. Lett.* **2009**, *34*, 827–829. [CrossRef]

27. Wang, Y.; Dai, X.; Wu, J.; Dinga, L.; Zeng, H. Spectral modulation of ultraviolet femtosecond laser pulse by molecular alignment of CO_2, O_2, and N_2. *Appl. Phys. Lett.* **2010**, *96*, 031105. [CrossRef]
28. Wilson, J.W.; Bartels, R.A. Rapid Birefringent Delay Scanning for Coherent Multiphoton Impulsive Raman Pump–Probe Spectroscopy. *IEEE J. Sel. Top. Quantum Electron.* **2012**, *18*, 130–139. [CrossRef]
29. Wang, C.H.; Jones, D.R.; Christensen, D.H. Studies of molecular motions of CH_2Br_2 in the liquid state by depolarized Rayleigh and Raman scattering. *J. Chem. Phys.* **1976**, *64*, 2820–2825. [CrossRef]
30. Kohmoto, T.; Fukuda, Y.; Kunitomo, M. Raman-induced rotational coherence in gaseous molecules observed by the ultrafast polarization spectroscopy. *Phys. Lett. A* **2000**, *277*, 233–239. [CrossRef]
31. Tamamitsu, M.; Sakaki, Y.; Nakamura, T.; Podagatlapalli, G.K.; Ideguchi, T.; Goda, K. Ultrafast broadband Fourier-transform CARS spectroscopy at 50,000 spectra/s enabled by a scanning Fourier-domain delay line. *Vib. Spectrosc.* **2017**, *91*, 163–169. [CrossRef]
32. Herzberg, G. Spectra of Diatomic Molecules. In *Molecular Spectra and Molecular Structure*; D. Van Nostrand Reinhold: Princeton, NJ, USA, 1950; Volume 1.
33. Knopp, G.; Beaud, P.; Radi, P.; Tulej, M.; Bougie, B.; Cannavo, D.; Gerber, T. Pressure-dependent N_2 Q-branch fs-CARS measurements. *J. Raman Spectrosc.* **2002**, *33*, 861–865. [CrossRef]
34. Knopp, G.; Radi, P.; Tulej, M.; Gerber, T.; Beaud, P. Collision induced rotational energy transfer probed by time-resolved coherent anti-Stokes Raman scattering. *J. Chem. Phys.* **2003**, *118*, 8223–8233. [CrossRef]
35. Linne, M.; Mecker, N.T.; Kliewer, C.J.; Escofet-Martin, D.; Peterson, B. Revisiting N_2-N_2 collisional linewidth models for S-branch rotational Raman scattering. *Combust. Flame* **2022**, *243*, 111928. [CrossRef]
36. Hellwarth, R.W.; Cherlow, J.; Yang, T. Origin and frequency dependence of nonlinear optical susceptibilities of glasses. *Phys. Rev. B* **1975**, *11*, 964–967. [CrossRef]
37. Zheltikov, A.M. An analytical model of the rotational Raman response function of molecular gases. *J. Raman Spectrosc.* **2008**, *39*, 756–765. [CrossRef]